Mechanochemical exfoliation and functionalization of MoS_2 in one step: a quick click method.

Marina Garrido,*[a]† Natalia Martín Sabanés[a] and Emilio M. Pérez*[a]

* Corresponding authors

[a] IMDEA Nanociencia, Faraday 9, 28049, Madrid, Spain. E-mail: emilio.perez@imdea.org, marina.garrido@uv.es

† Current address: Instituto de Ciencia Molecular (ICMol), Universitat de Valencia, Carrer del Catedrátic José Beltrán Martínez 2, 46980, Paterna, Valencia, Spain

Supplementary Information

1. Materials and methods

All reagents were purchased from commercial sources and used without further purification. *N*-benzylsuccinimide was synthesized using a previously reported procedure.[1] Molybdenum disulfide (MoS_2, 98%, particle size < 2 μm) was purchased from Sigma-Aldrich. *N*-Benzylmaleimide (purity > 98%) was obtained from TCI Europe. 1-Dodecyl-1H-pyrrole-2,5-dione (purity > 95%) and *N*-(2-aminoethyl)maleimide hydrochloride (purity 96%) were purchased from BLDpharm. Vacuum filtrations of MoS_2 materials were carried out with polytetrafluoroethylene (PTFE) (pore size = 0.2 μm, Φ = 25 mm) membranes.

Optimized exfoliation procedure:

30 mg of MoS_2 and 2.5 mmol of the appropriate maleimide were placed in a 20 mL stainless steel reactor containing 8 stainless steel balls (Φ = 10 mm). The reactor was introduced in a Fritsch Planetary Micro Mill PULVERISETTE 7, and the mixture was milled at 600 rpm for 10 min at RT and under Ar atmosphere. After the milling, the obtained material was recovered in two fractions: 1) powder, subsequently dispersed in the appropriate solvent and 2) directly dispersed in that solvent. Both fractions were centrifuged (Allegra X-15R centrifuge, Beckman Coulter, FX6100 rotor) at 1000 rpm for 30 min at 20 ˚C several times to separate the exfoliated MoS_2 from the bulk one. The green supernatant from both fractions was vacuum filtered and cleaned by several cycles of redispersion/filtration in the appropriate solvent (ACN for *N*-benzylmaleimide and dodecyl-1H-pyrrole-2,5-dione and distilled water for *N*-(2-aminoethyl)maleimide hydrochloride)) to remove the free maleimide affording functionalized MoS_2 in powder.

As a control experiment this procedure was performed but in the absence of maleimide.

To study the role of the molecule in the developed method, the optimized exfoliation procedure was carried out in the presence of *N*-benzylsuccinimide.

2. Instruments

UV-Vis spectroscopy

UV-Vis measurements were carried out on a Cary 5000 UV-Vis-NIR spectrophotometer (Agilent Technologies), using 1 cm path quartz cuvettes. For dispersibility measurements, R-succ-MoS_2 were dispersed in ACN, IPA, EtOAc, acetone and water by sonicating 1 min 0.5 mg of R-succ-MoS_2 in 5 mL of the desired solvent.

Raman spectroscopy

Bulk MoS_2 was measured in powder onto a glass slide. Bn-succ-MoS_2 and control MoS_2 samples were prepared by spin-coating on silicon surfaces and were dried under vacuum overnight. Raman measurements were performed using a commercial confocal Raman microscope (Senterra II, Bruker). The spectra were acquired using 633 nm wavelength, 5 mW, 4 second acquisition, 10 coadquisitions, 9-15 cm^{-1} resolution using a 100X Olympus objective.

Transmission electron microscopy (TEM)

TEM images were obtained using a JEOL JEM 2100 operated at 200 kV. The samples were dispersed in ACN and dropped onto a holey carbon copper grid (200 mesh), the solvent was removed at room temperature overnight.

Atomic force microscopy (AFM)

AFM was carried out under ambient conditions using a commercial AFM system (Ntegra Prima, NT-MDT) in semicontact (dynamic) mode with a pyramidal silicon tip (HQ:NSC14/Al BS probes from MikroMasch) at a working frequency of 160 kHz and a nominal force constant of 5 N/m. The samples were prepared by spin-coating on silicon surfaces and were dried under vacuum overnight.

Thermogravimetric analysis (TGA)

TGA measurements were performed in a TGA Q550 (TA Instruments) under Air atmosphere. The samples were introduced inside a platinum crucible and equilibrated at 100 ˚C followed by a 10 ˚C/min ramp between 100 and 850 ˚C.

Diffuse reflectance infrared Fourier transform (DRIFT) spectroscopy

DRIFT spectra were carried out in a Bruker ALPHA spectrometer equipped with a diffuse reflectance module using a spectral range of 4000-400 cm^{-1}, with a resolution of 4 cm^{-1}. The samples were prepared by grinding the powder of the desired compound in a KBr (Scharlau, IR spectroscopy grade) matrix. The KBr baseline was subtracted from the spectra.

Solid-state CP-MAS-^{13}C-NMR

Solid-state CP-MAS-^{13}C-NMR spectra were recorded on a Bruker AV 400 WB spectrometer.

X-ray photoelectron spectroscopy (XPS)

XPS measurements were performed in a SPECS FIeXPS spectrometer under Ultra High Vacuum conditions (UHV, 1-3x10^{-10} mbar), using a monochromatic Al Kα line as exciting photon source (1486.71 eV, 300 W). The emitted photoelectrons were collected in a PHOIBOS 150 AD-CMOS energy analyzer (pass energy 20 eV, step 1eV for survey spectra, step 0.1 eV for high resolution spectra). To compensate the built up charge on the sample surface it was necessary to use a Flood Gun (3 V and 40 μA). The fitting of the spectra was carried out using CasaXPS software.

3. Supporting Images and Tables

Table S1: Tested conditions for simultaneous exfoliation and functionalization of MoS_2.

Entry	MoS_2 (mg)	*N*-benzylmaleimide (mg)	Solvent	Balls	rpm	Time
1	30	468	ACN	4 (Φ = 15mm)	600	60' (10', 15' pause) x6
2	30	468	ACN	8 (Φ = 10mm)	600	60' (10', 15' pause) x6
3	30	468	No	8 (Φ = 10mm)	600	60' (10', 15' pause) x6
4	30	468	No	8 (Φ = 10mm)	600	10'
5	30	468	No	8 (Φ = 10mm)	450	10'
6	30	468	No	8 (Φ = 10mm)	300	10'
7	30	468	No	8 (Φ = 10mm)	150	10'
8	30	468	No	8 (Φ = 10mm)	600	1'
9	30	473 (*N*-benzylsuccinimide)	No	8 (Φ = 10mm)	600	10'

From the UV-Vis spectra (Figure S1a), it could be determined that under all tested conditions MoS_2 was exfoliated in the presence of *N*-benzylmaleimide, except for entry 1 (Table S1). Entry 2 afforded exfoliated MoS_2 (Figure S1a). However, the number of layers is higher than the one obtained when the milling was dry performed (Table S2).

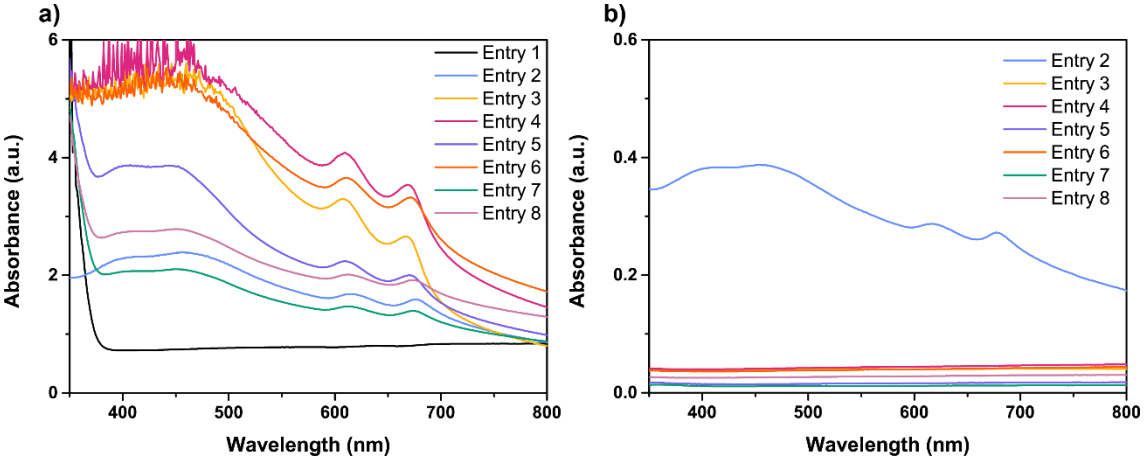


Figure S1: a) UV-Vis supernatant spectra of powder fraction in ACN of MoS_2 milled in the presence of *N*-benzylmaleimide and b) UV-Vis supernatant spectra of powder fraction in ACN of MoS_2 milled in the absence of *N*-benzylmaleimide.

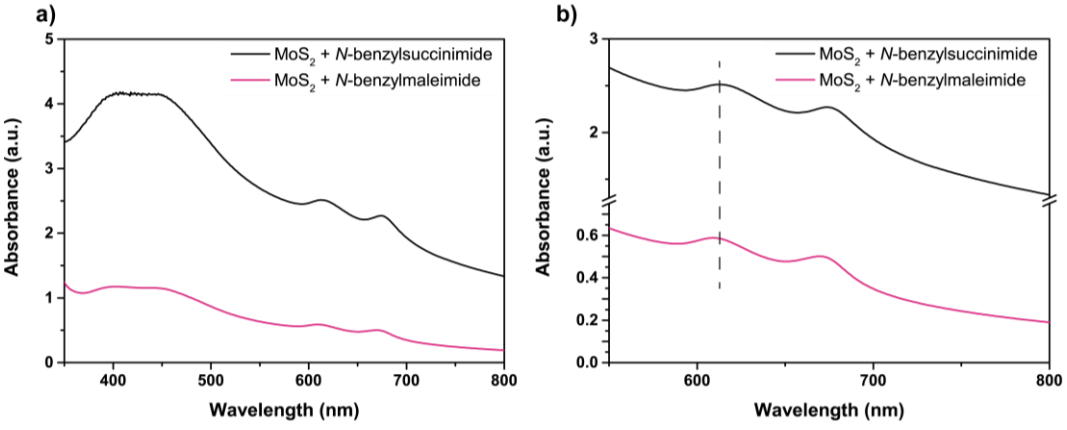


Figure S2: a) UV-Vis supernatant spectra of MoS_2 milled in the presence of *N*-benzylmaleimide (Entry 4) and in the presence of *N*-benzylsuccinimide (Entry 9). b) Zoom in the region between 550-800 nm.

Table S2: Position and absorbance of excitons A and B for all tested conditions. Number of layers of MoS_2 calculated from the position of exciton A.

Entry	Exciton A (nm)	Absorbance exciton A	Number of layers	Exciton B (nm)	Absorbance exciton B
1	707	0.83	Bulk	640	0.80
2	676	1.59	12	615	1.68
3	667	2.66	4	607	3.29
4	669	3.54	5	609	4.08
5	669	2.00	5	609	2.24
6	671	3.32	6	611	3.65
7	673	1.39	8	613	1.47
8	673	1.92	8	612	2.01
9	674	2.27	9	613	2.51

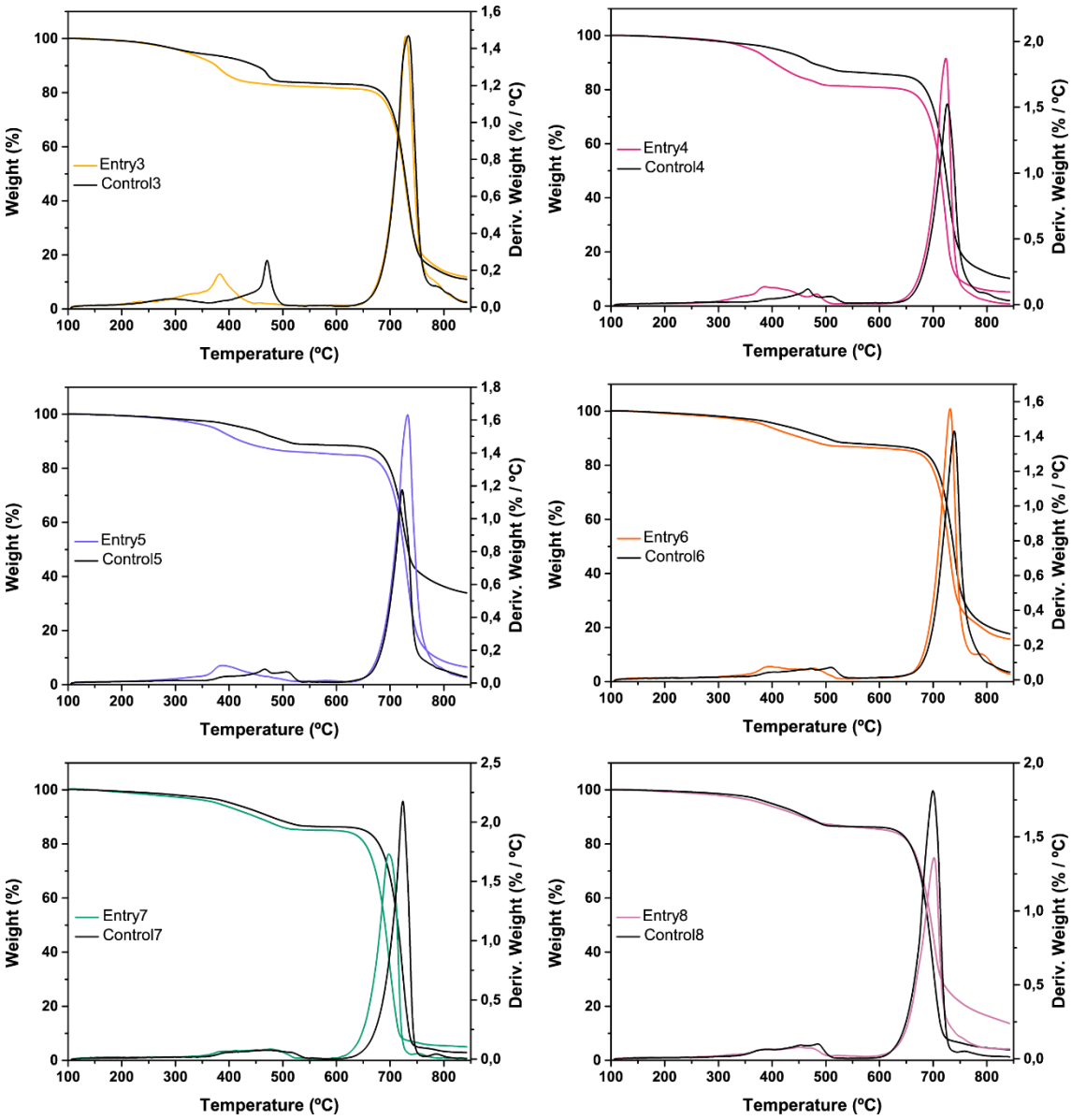


Figure S3: TGA weight loss of functionalized MoS_2 with *N*-benzylmaleimide employing different reaction conditions. The black curves correspond to the respective control experiments.

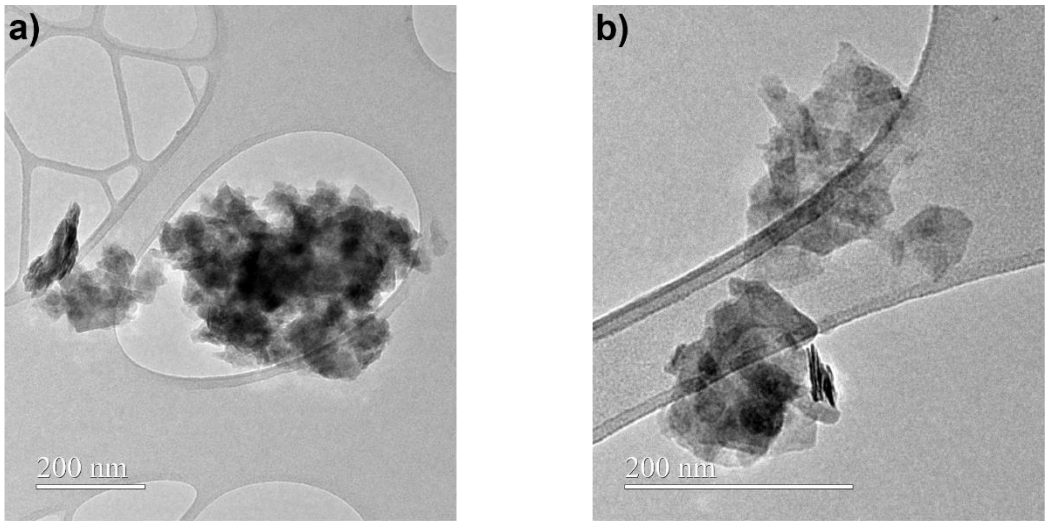


Figure S4: Representative TEM images of Bn-succ-MoS_2 obtained using the conditions of Entry 3 (Table S1).

Despite the exfoliation efficiency of Bn-succ-MoS_2 after 1h of milling is slightly better than after 10 minutes (Table S1 and S2), the functionalization degree is not highly affected by the time (Fig. S2). In addition, the lateral dimensions of the obtained flakes clearly diminish, implying a higher damage of the material.

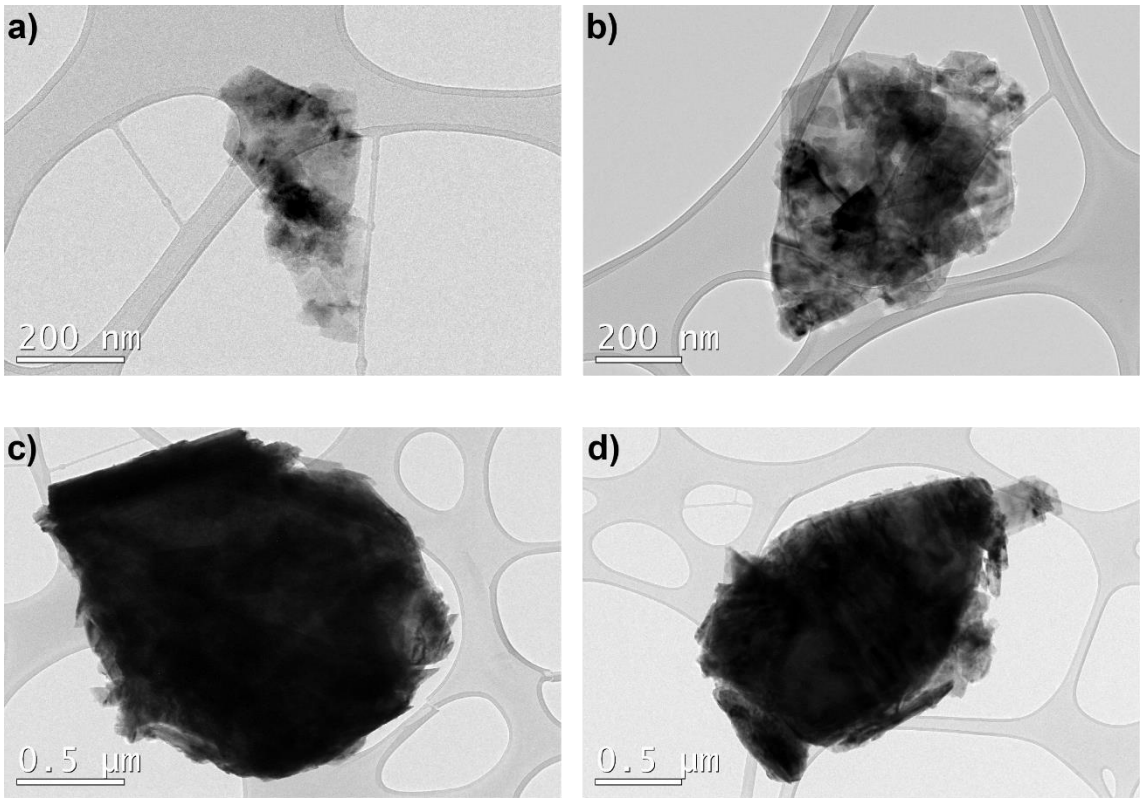


Figure S5: a) and b) Representative TEM images of Bn-succ-MoS_2. c) and d) Representative TEM images of control MoS_2 (milled in the absence of *N*-benzylmaleimide).

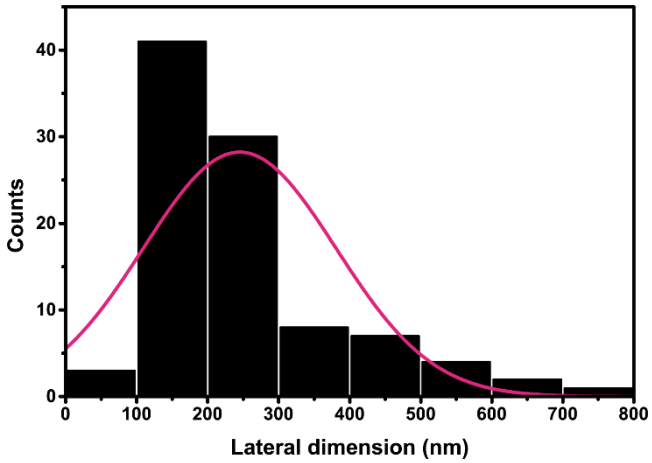


Figure S6: Lateral dimension distribution of Bn-succ-MoS_2 from TEM images.

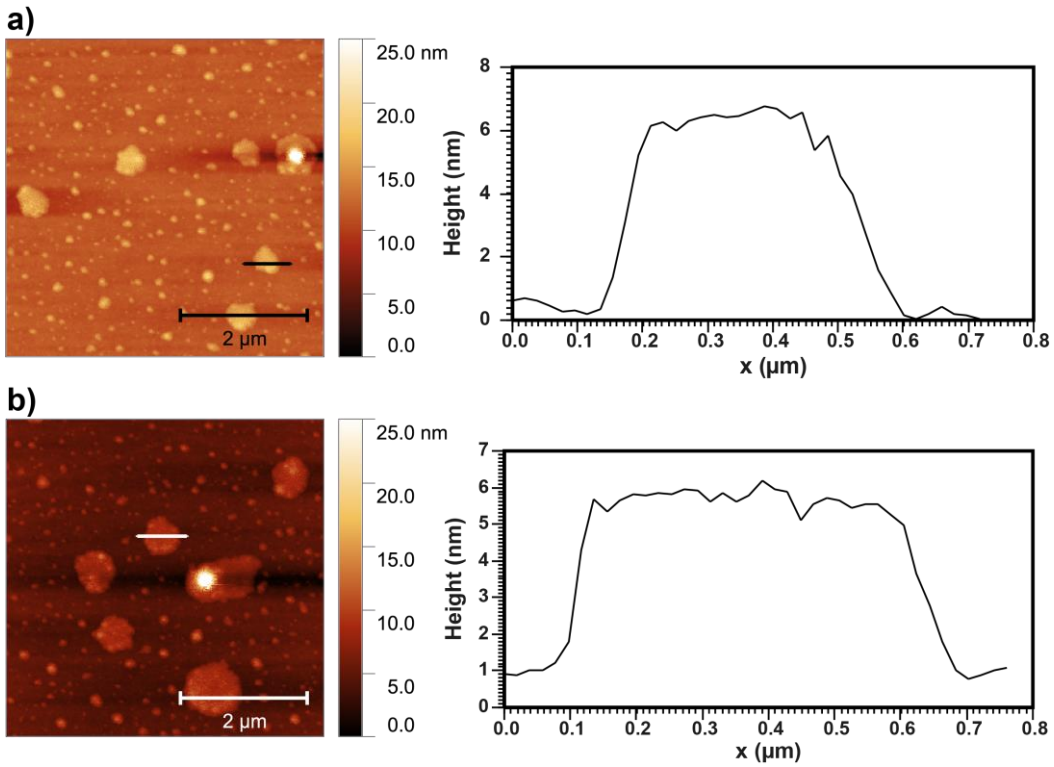


Figure S7: a) and b) Representative AFM images of Bn-succ-MoS_2 and their corresponding height profile.

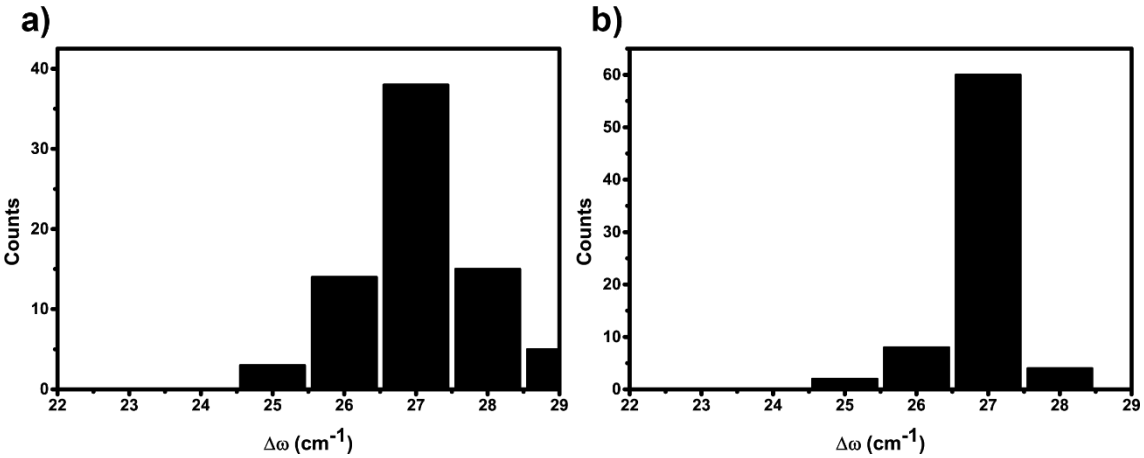


Figure S8: a) and b) Δω distribution of bulk MoS_2 and control MoS_2 (milled in the absence of *N*-benzylmaleimide), respectively.

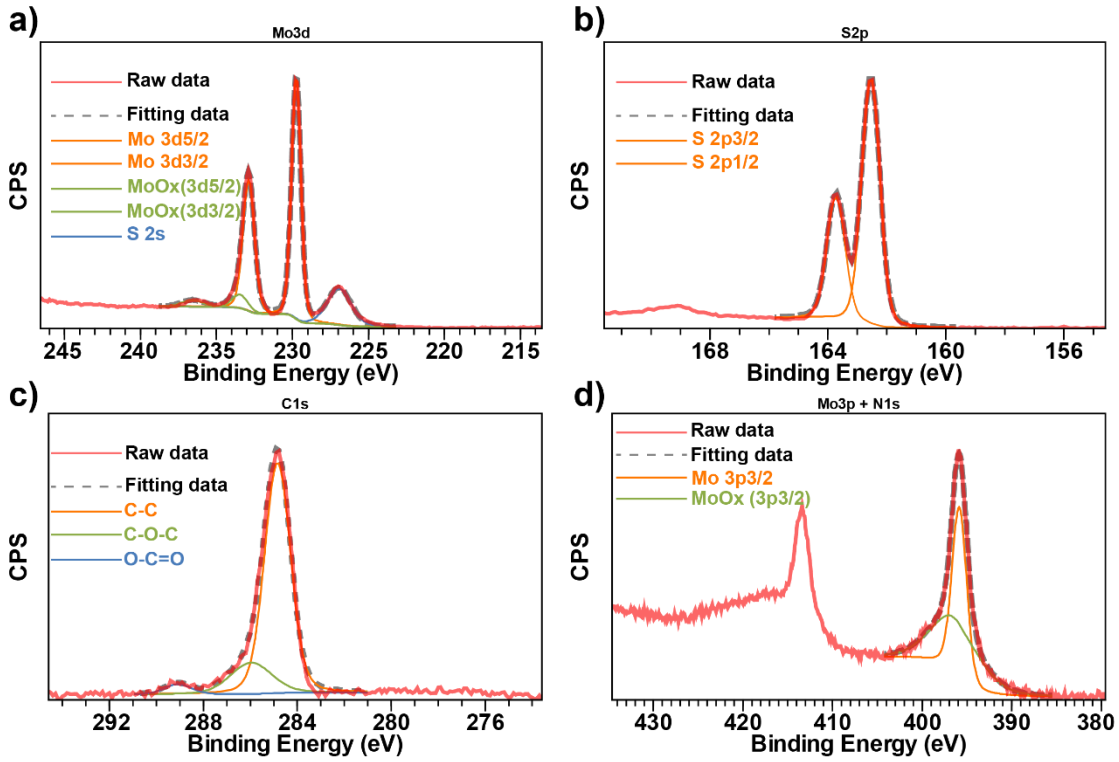


Figure S9: XPS spectra of a) Mo, b) S, c) C and d) N core levels for bulk MoS_2.

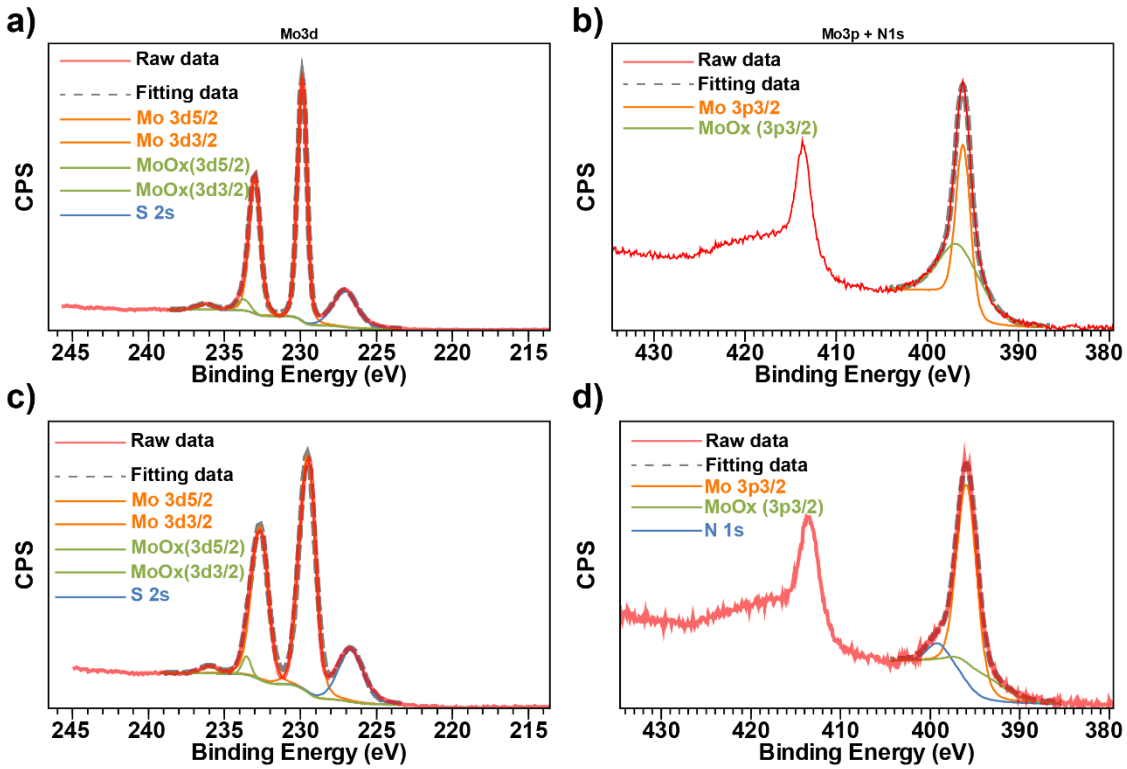


Figure S10: a-b) XPS spectra of Mo and N core levels for control MoS_2. c-d) XPS spectra of Mo and N core levels for Bn-succ-MoS_2.

Table S3: Mo3d, S2p, C1s, Mo3p and N1s core level components for bulk MoS_2, control MoS_2 and Bn-succ-MoS_2.

Sample	Component	Binding Energy (eV)	Atomic %
Bulk MoS_2	Mo 3d5/2	229.7	45.5
	Mo 3d3/2	232.9	30.0
	MoOx (3d5/2)	233.4	4.3
	MoOx (3d3/2)	236.6	2.8
	S 2s	226.9	17.4
	S 2p3/2	162.5	66.7
	S 2p1/2	163.7	33.3
	C-C	284.8	79.4
	C-O-C	286.0	17.1
	O-C=O	289.1	3.5
	Mo 3p3/2	395.8	48.6
	MoOx (3p3/2)	396.2	51.4
Control MoS_2	Mo 3d5/2	229.9	46.7
	Mo 3d3/2	233.0	30.8
	MoOx (3d5/2)	233.7	2.8
	MoOx (3d3/2)	236.3	1.9
	S 2s	227.1	17.8
	S 2p3/2	162.6	66.7
	S 2p1/2	163.8	33.3
	C-C	284.9	65.3
	C-O-C	286.0	25.2
	O-C=O	288.1	9.5
	Mo 3p3/2	396.0	48.6
	MoOx (3p3/2)	396.1	51.4
Bn-succ-MoS_2	Mo 3d5/2	229.5	48.4
	Mo 3d3/2	232.7	31.9
	MoOx (3d5/2)	233.5	2.0
	MoOx (3d3/2)	236.0	1.3
	S 2s	226.7	16.4
	S 2p3/2	162.0	36.9
	S 2p1/2	163.2	18.5
	S-C	162.8	29.7
	S-C	163.9	14.9
	C-C	284.7	66.6
	C-N	285.8	27.7
	C=O	288.7	5.7
	Mo 3p3/2	395.9	72.1
	MoOx (3p3/2)	394.4	19.9
	N 1s	399.1	8.0

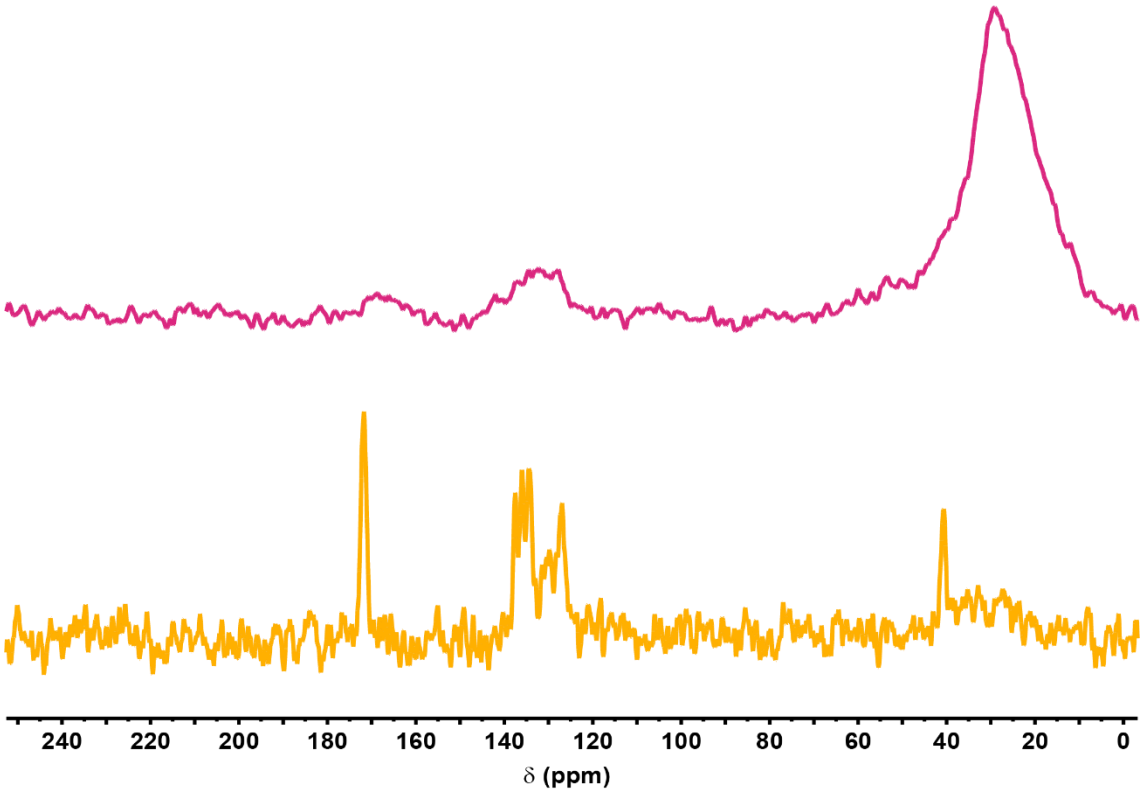


Figure S11: Solid-state CP-MAS-^{13}C-NMR spectra of *N*-benzylmaleimide (yellow) and Bn-succ-MoS_2 (pink).

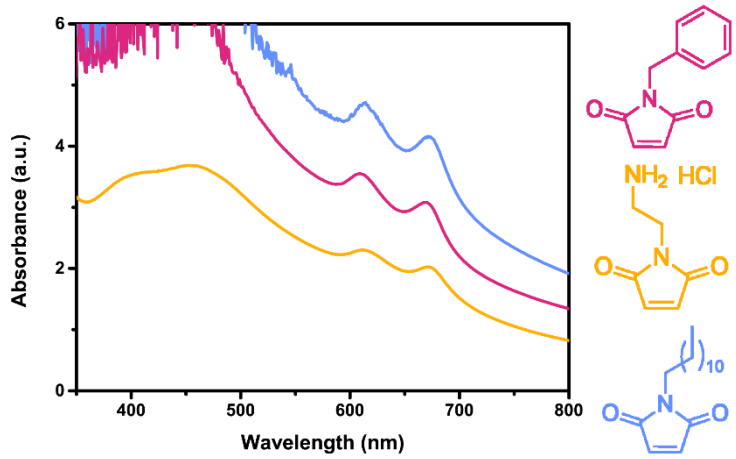


Figure S12: UV-Vis supernatant spectra of powder fraction of MoS_2 milled in the presence of *N*-benzylmaleimide (ACN), *N*-(2-aminoethyl)maleimide hydrochloride (water) and *N*-dodecylmaleimide (ACN).

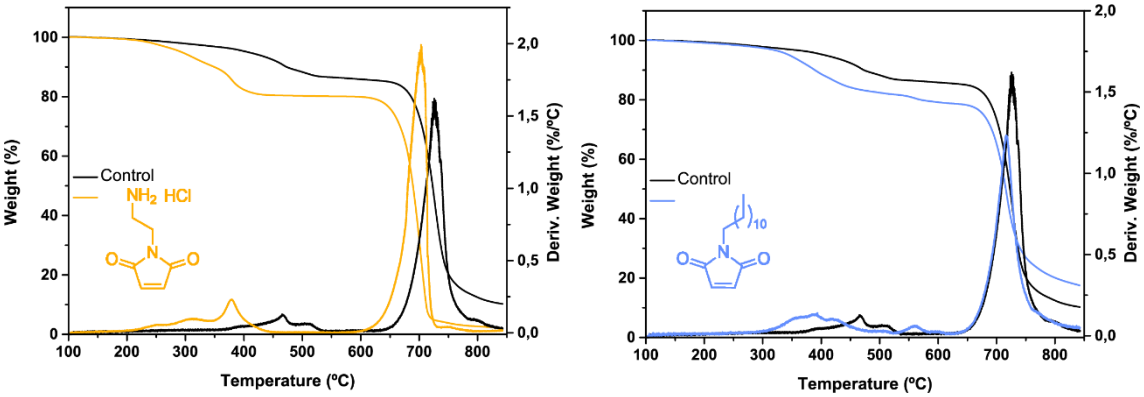


Figure S13: TGA weight loss of functionalized MoS_2 with *N*-(2-aminoethyl)maleimide hydrochloride and *N*-dodecylmaleimide. The black curve corresponds to the control experiment.

$$Weight\ loss\ (\%) = \frac{X \times MW\ (Moiety\ attached)}{X[MW(Moiety\ attached) + MW(MoS_2)] + (1 - X) \times MW(MoS_2)} \times 100$$

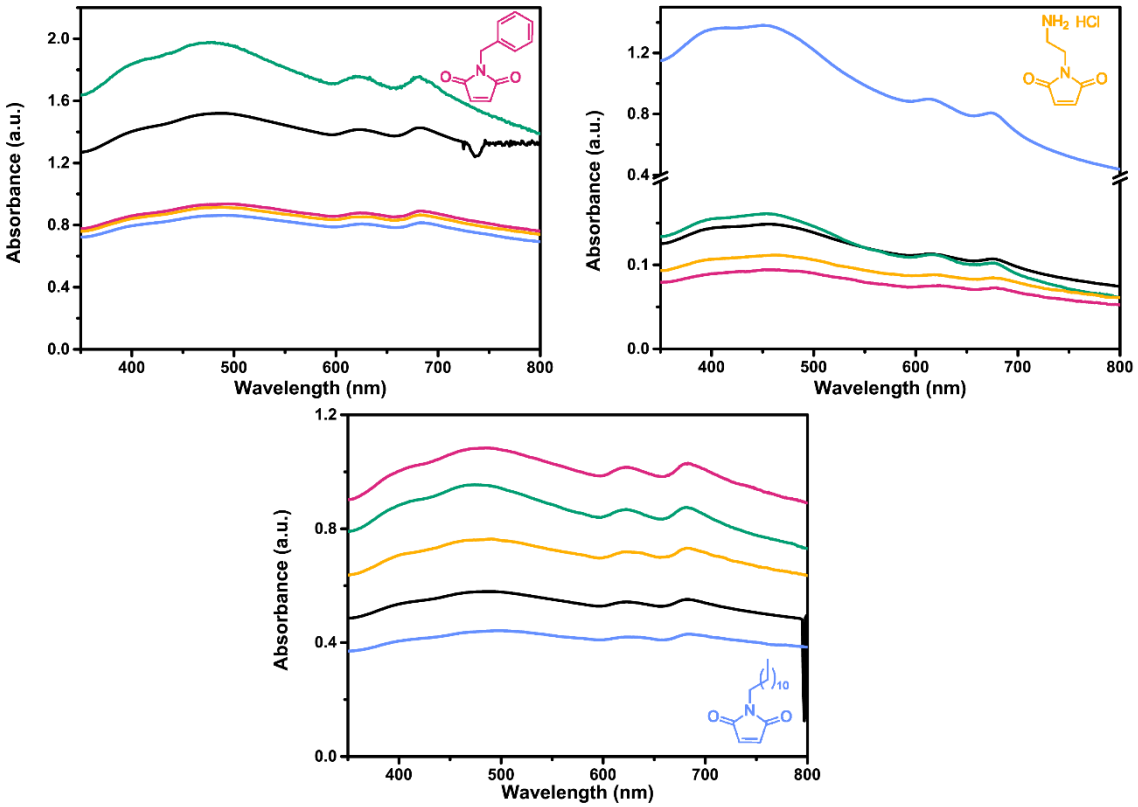


Figure S14: UV-Vis spectra of Bn-succ-MoS_2, NH_2-succ-MoS_2 and dodecyl-succ-MoS_2 in ACN (black), IPA (green), EtOAc (pink), acetone (yellow) and water (blue).

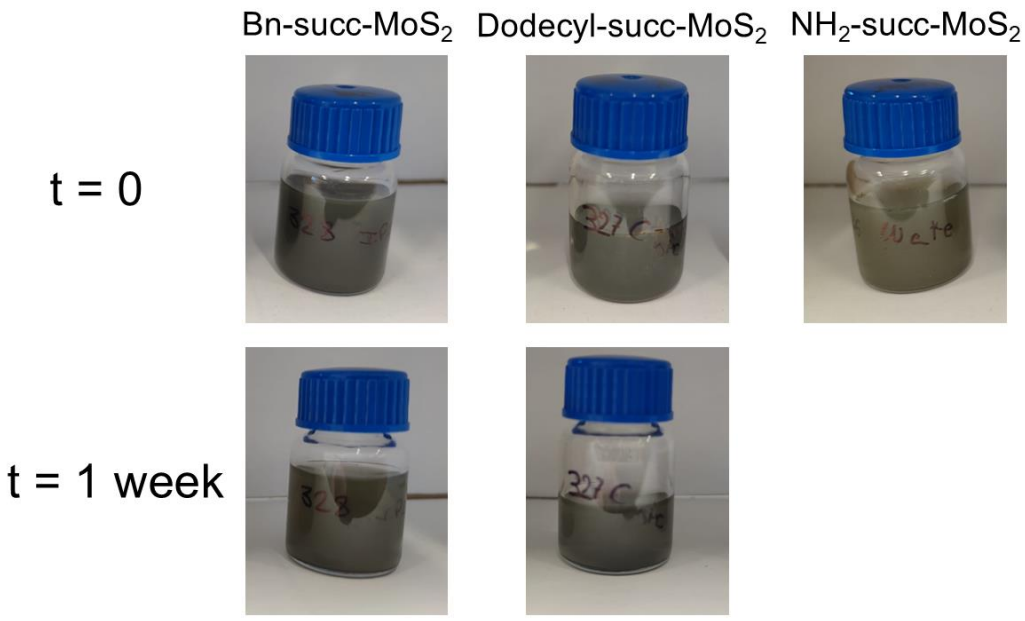


Figure S15: Dispersions of Bn-succ-MoS_2 (IPA), dodecyl-succ-MoS_2 (EtOAc) and NH_2-succ-MoS_2 (water) at t= 0 and after 1 week.

Table S4: Summary of several one-step exfoliation and functionalization methods and other exfoliation approaches for MoS_2.

Method	Time	Exfoliation yield (%)	TGA weight loss (%)	Scalability	Lateral dimension (nm)	Thickness (nm)	Ref
Ball-mill one-step	10 min	47	5	Possible	245 ± 136	5 ± 1	This work
Ultrasonic bath one-step	6 days	Not reported	8.5	Possible	100-700	3.3 (one flake)	2
Electrochemical one-step	30 min	Not reported	Not reported	Possible	~ 500	~ 4	3
Ball-mill	6 h	94	—	Possible	~ 80	Not reported	4
Ball-mill	15 min	82.9	—	Possible	290 ± 114	Not reported	5
Ball-mill	8 h	92	—	Possible	2.4 ± 0.1 μm	4.27 ± 0.12	6
Bath sonicator	4 h	52	—	Possible	~ 500	~ 6	7
Electrochemical	1 h	70	—	Possible	5-50 μm	3.9-6.7	8
Microwave irradiation	90 s	34	—	Yes	1.2 ± 0.7 μm	4 ± 2	9
Ball-mill (two steps)	24h + 24h	66.7% (exf.)	28	Possible	197 ± 25 (exf.) 133 ± 70 (fun.)	3.8 ± 0.9 (exf.) 2.5 ± 1.2 (fun.)	10

References:

1 Z.-G. C. Le Zhen-Chu; Hu, Yi; Zheng, Qin-Guo, *Synthesis*, 2004, **2004**, 995–998.

2 R. H. Gonçalves, R. Fiel, M. R. S. Soares, W. H. Schreiner, C. M. P. Silva and E. R. Leite, *Chem. – A Eur. J.*, 2015, **21**, 15583–15588.

3 Y. Zhuo, I. A. Kinloch and M. A. Bissett, *ACS Appl. Nano Mater.*, 2023, **6**, 18062–18070.

4 A. Tayyebi, N. Ogino, T. Hayashi and N. Komatsu, *Nanotechnology*, 2020, **31**, 75704.

5 V. J. González, A. M. Rodríguez, I. Payo and E. Vázquez, *Nanoscale Horizons*, 2020, **5**, 331–335.

6 R. Navik, H. Tan, H. Zhang, L. Shi, J. Li and Y. Zhao, *Small Methods*, 2024, **8**, 2301334.

7 G. D'Olimpio, J. Occhiuzzi, L. Lozzi, L. Ottaviano and A. Politano, *Adv. Sustain. Syst.*, 2022, **6**, 2200277.

8 P. Zhang, S. Yang, R. Pineda-Gómez, B. Ibarlucea, J. Ma, M. R. Lohe, T. F. Akbar, L. Baraban, G. Cuniberti and X. Feng, *Small*, 2019, **15**, 1901265.

9 R. Quirós-Ovies, M. Laborda, N. M. Sabanés, L. Martín-Pérez, S. M.-D. Silva, E. Burzurí, V. Sebastian, E. M. Pérez and J. Santamaría, *ACS Nano*, 2023, **17**, 5984–5993.

10 T. Umeyama, D. Mizutani, Y. Ikeda, W. R. Osterloh, F. Yamamoto, K. Kato, A. Yamakata, M. Higashi, T. Urakami, H. Sato and H. Imahori, *Chem. Sci.*, 2023, **14**, 11914–11923.